Research Journal of Applied Sciences 7 (9-12): 435-443, 2012
ISSN: 1815-932X

Design of Anisogrid Composite Lattice Conical Shell Structures

[1]Jafar Eskandari Jam, [1]Milad Noorabadi, [2]S.H. Taghavian,
[2]Mohammad Reza Asadi Asad Abad and [1]Nader Namdaran
[1]Composite Materials and Technology Center, Tehran, Iran
[2]Department of Mechanical Engineering, Buinzahra Branch,
Islamic Azad University, Buinzahra, Iran

Abstract: Lattice structures due to their low weight and high performance as structural elements have been widely used in different aerospace applications. In this study, effective parameters on the design of anisogrid lattice conical shells are investigated. First, filament winding patterns regarding the desired axial strength is decided. Then, regarding geometrical relations, effective parameters in order to form the anisogrid cell are identified. Distance of circular ribs from each other has an important role in determining the conical lattice structure and eventually in deriving the stiffness matrix. Finally, considering the relations, Finite Element Analysis Model of the lattice conical structure has been performed by ABAQUS software and buckling analysis under axial loading is done. In deriving the strength results, the verifications of references of this study and the classic theory have been used.

Key words: Rib, stiffness matrix, lattice structure, finite element, strength, Iran

INTRODUCTION

Composite lattice structures are one of the most complex and newest structures which are designed and produced in both isogrid and anisogrid forms. In the past decade, researches done on polymeric matrix fiber composite lattice structures have become one of the scientific and widely used centers of attention and these structures have a widespread application in different aerospace structures. These structures as lattice lamina are used lonely or with internal or external shells. Lattice lamina in these structures includes different systems of ribs which are produced from continuous fibers using automatic filament winding method. In these structures under arbitrary loading fibers of the lattice are under tension or compression which is a quite desirable state for composites and is one of the major advantages of these structures compared to the conventional structures for composites. Major characteristics of these composites in the face of axial compression and bending moment loadings are different failures occurring due to total buckling of the structure, failure due to maximum stress in helical ribs and failure due to local buckling of the helical ribs in the lattice. Buckling load related to each of the failure states depends upon geometric parameters and total dimensions of the structure. In the analysis of these structures it is supposed that elements of the lattice are two force members behaving as an orthotropic body and the relations of orthotropic structures are used here for the analysis of the total buckling of these structures. Major application of these structures is in aerospace industry which widely uses different forms of them including: curved shaped and annular shells (especially conical shells). For the purpose of improving the mechanical properties of the structure and its weight optimization, composite materials have been used. In the midst of 1960's the finite element method was developed for the numerical analysis of these structures. Generally, these structures are manufactured y advanced forming of fibers. Also, the ribs use in these structures can move in 2 up to 4 directions. Design, analysis and manufacture of these structures are investigated in reference (Huybrechts and Meink, 1999a, b). More details of their analysis are included in references (Huybrechts and Meink, 1996, 1999a, b). In references (Wodesenbet *et al*., 2003; Kidane *et al*., 2003), buckling load analysis of grid stiffened cylindrical shells is performed. Also, the results of the experimental test are compared and verified in comparison with the analytical results. Kim (1999, 2000) has studied the fabrication and testing of thin composite isogrid stiffened panels and composite isogrid stiffened cylinders, so as to investigate their buckling behavior. In reference (Goldfeld *et al*., 2005) design and optimization of laminated conical shells for buckling and maximum buckling loads has been performed. In this study, optimization has been performed in two states of causing

Corresponding Author: Jafar Eskandari Jam, Composite Materials and Technology Center, Tehran, Iran

the maximum buckling load at certain weight and causing the minimum weight under a constant critical load. In the study (Goldfeld and Arbocz, 2004), critical buckling load is derived from the solution of the governing nonlinear partial differential equation with different coefficients. Blom *et al*. (2007) has investigated the optimized stacking sequence design, so as to achieve the maximum fundamental eigenfrequency in conical shells. In the study (Morozov *et al*., 2011) buckling of the cylindrical lattice structure has been done, using Finite Element Method. Also, in study (Morozov *et al*., 2011) finite element analysis for buckling of the conical lattice shell is studied. In this study, a numerical code is developed for the conical lattice structure which determines the basic parameters, buckling under critical axial loading, torsion moment and bending moment. In this study, design of the conical lattice structure with the anisogrid cell is investigated. First, the governing differential equations of the anisogrid cell of the conical lattice structure are derived, regarding the filament winding technique used. Then, variations of the principal parameters of the design are investigated in relation to the increase of the number of helical rib. Later by creating a Finite Element Model of the conical lattice structure with the anisogrid cell, buckling analysis of the structure under axial loading is performed. Also, the variations of the critical buckling load, relative to increase of thickness, width and the distance between ribs is considered.

MATERIALS AND METHODS

Governing equations of design: Lattice structures are widely used in different industries. These structures are highly strong against the destruction caused by impact, delamination and craze propagation in the structure. One of their advantages over other structures is reduction of weight and manufacture time. Lattice structure is made of a number of helical and circular ribs. These structures can have up different forms including isogrid and anisogrid. Generally, the main purpose of using lattice structures is optimal usage of longitudinal properties of the composite materials used. Also, a schematic of the conical lattice shell used as a satellite carrier adaptor, at the lower section of the satellite is shown in Fig. 1.

All the parameters are determined on the basis of the location of helical and circular ribs. Some of these parameters depend on the angel of the helical ribs. Also, some of these parameters as the height of the structure increases have variations with a certain rate. Because of the complexity of the geometry of conical lattice shells, in order to design, one first must divide the effective design parameters of the structure in two dependent and independent categories and then perform the complete investigation procedure of design.

Independent parameters: The number of circular and helical ribs (n_c, n_h) are independent parameters in the design of conical lattice structure.

Dependent parameters: Dependent parameters include: $\Delta\psi$, φ, λ, a_c, a_h. A schematic of the parameters stated here in the design of annular lattice structure is shown in Fig. 2.

Since, the design of these structures is intended to stand axial compression loadings, therefore the most important problem regarding these structures is the analysis of buckling and elastic stability. Considering these facts, design of the lattice structure and eventually manufacture of it, must be based on a state that shows the maximum strength against buckling. Amongst different filament winding patterns, geodesic pattern is the best

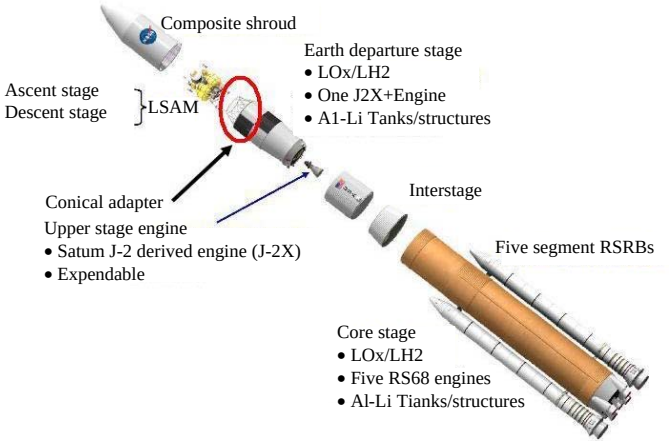

Fig. 1: A schematic of the satellite carrier adaptor (Balepin *et al*., 2000)

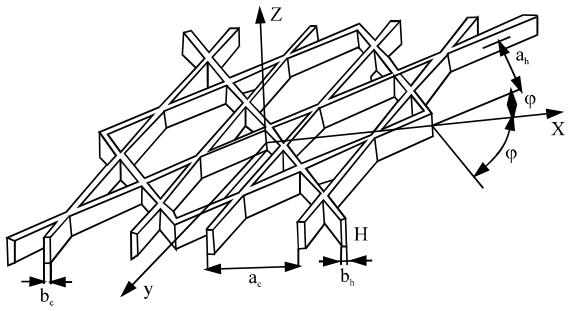

Fig. 2: Geometric parameters of the lattice structure

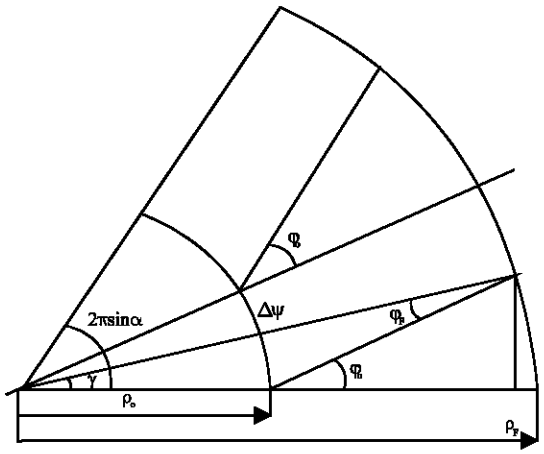

Fig. 3: Developed section of the conical lattice shell

pattern of filament winding for lattice structures, carrying axial compression loadings. In order to derive the governing differential equations of the structure, first by developing a section of the cone, the geometric equations which have a direct effect on the stiffness matrix are achieved (Fig. 3). Using geodesic relations, the following equation for each point of the lattice structure exists (Kim, 2000):

$$\rho\sin\varphi = \rho_0\sin\varphi_0 = C_0 = \text{constant} \quad (1)$$

Wherein $$\rho = \frac{r}{\sin\alpha}$$

and r is the radius of the cross section of the cone which is different at each point and α is the angle between the line passing through the apex of the cone and the axis of symmetry of the cone. Taking derivation of Eq. 1 gives:

$$\frac{d\rho}{\rho} = -\frac{d\varphi}{\tan\varphi} \quad (2)$$

where, Δψ is the angle between the two helical ribs of Fig. 3 and is found here:

$$\Delta\psi = \frac{2\pi\sin\alpha}{n_h} \quad (3)$$

Geometrical design and finite element analysis of the conical lattice structure is performed with the assumption that the circular ribs are located between the intersection of the helical ribs. Considering the geometry of Fig. 3, the following equation is achieved:

$$\gamma = \frac{\Delta\psi}{2}(n_c - 1) \quad (4)$$

Geodesic angle at the smaller cross-section (φ_0) is computed as follows:

$$\varphi_0 = \tan^{-1}\left(\frac{\rho_F \sin\gamma}{\rho_F\cos\gamma - \rho_0}\right) \quad (5)$$

And also, the geodesic angle at the bigger cross-section (φ_0) is equal to:

$$\varphi_F = \varphi_0 - 1 \quad (6)$$

Variations of ρ versus φ are achieved by this equation:

$$d\rho = -C_0\frac{\cos\varphi}{\sin^2\varphi}d\varphi \quad (7)$$

Vertical space between circular and helical ribs for a cell at each row is derived from the following equations:

$$a_h = 2a_c\sin\varphi \quad (8)$$

$$(a_c)_{i,i+1} = -\frac{\int_{\rho_i}^{\rho_{i+1}}\Delta\psi d\rho}{\int_{\varphi_i}^{\varphi_{i+1}}2d\varphi} \quad (9)$$

In Eq. 9, i indicates the number of ribs. The minus sign in Eq. 9 shows that the axis of the system of coordinate system is located on the smaller cross-section. Stiffness properties of one cell which has a repeating pattern is the representative of the total repeating section. The orthotropic properties achieved for annular bodies is along the axial direction. For example for the cylindrical structure, stiffness along the axial direction is equal to:

$$\overline{E}_x\frac{A}{L}$$

where, A = 2πRH is the cross-section of the structure.

$$[Q]=\begin{bmatrix} \frac{2E_h b_h c^4}{a_h} & \frac{2E_h b_h}{a_h}s^2c^2 & 0 \\ \frac{2E_h b_h}{a_h}s^2c^2 & \frac{2E_h b_h}{a_h}s^4+\frac{E_c b_c}{a_c} & 0 \\ 0 & 0 & \frac{2E_h b_h}{a_h}s^2c^2 \end{bmatrix} \quad (10)$$

$$s=\sin\varphi, c=\cos\varphi$$

E_h and E_c are the moduli of elasticity of helical and circular ribs, respectively. Equation 10 is directly derived from theory, formulation and assumptions which are related to the stiffness of the layer and the properties of fibers. Also, properties of the equal stiffness along the axial direction are derived from Eq. 11 (Kim, 2000):

$$\bar{E}_x = \frac{1}{H}\left(\frac{q_{11}q_{22}-q^2_{12}}{q_{22}}\right) \quad (11)$$

q_{ij} used in Eq. 11 are the components of the stiffness matrix Q and as it is seen, they depend upon the angle of helical ribs, width of the ribs and the distance between helical and circular ribs. The critical buckling axial load for conical shell is given by Weingarten *et al.* (1965):

$$P_{cyl\infty} = \frac{2\pi\bar{E}_x t^2}{\sqrt{3(1-\nu^2)}}\cos^2\alpha \quad (12)$$

According to Eq. 12, the critical buckling axial load for conical shells is the same as that of cylindrical shells with this difference that the angle for half-apex of the cone is also effective in the critical load. By comparison of the experimental, analytical and finite element analysis, it is found out that in order for the analytical result to have an acceptable answer, a buckling correction factor of C must be multiplied with it. Eventually by applying the buckling correction factor, the critical buckling load of the conical shell is equal to:

$$P_{cyl\infty} = C\frac{2\pi\bar{E}_x t^2}{\sqrt{3(1-\nu^2)}}\cos^2\alpha \quad (13)$$

According to Weingarten *et al.* (1965), the magnitude of parameter C depends on the angle of the cone's inclination. The correction factor of C for a cone having the apex angle of 10 up to 75° is equal to 0.33. At a range outside these angles, C is derived according to experimental test.

FINITE ELEMENT MODEL

Regarding the fact that these structures cannot be transformed into smaller samples, in order to determine the mechanical specification of the structure, one can only use the possible solution of experimental test. Numerical analysis of the lattice structure is performed using Timoshenko's beam element and the shell's element as it is seen in Fig. 4. Generally, considering the situation that major loads applied to the lattice structure are axial loads, therefore buckling is the most important parameter in strength evaluation of these structures. Choosing of the beam element is described in reference (Morozov *et al.*, 2011). Circular and circumferential ribs of the lattice structure are completely bonded to each other at the intersection points. The distance between circular and helical ribs from each other is achieved, considering the governing relations.

In order to design the winding pattern of the fibers, it is necessary to derive the geodesic angles of the helical ribs in big and small cross-sections and the height location of the conical structure should be known. For the design of conical lattice structure and regarding Eq. 6, 7 and 10 the total dimensions including height, bigger and smaller cross-sections and the apex angle must be determined. By this explanation, big and small diameters of the cone are 2500 and 1250 mm, respectively and the apex angle is 34.7°. Now, regarding the geometric specification stated, geodesic angle variations at different height locations sand different number of circular ribs is derived. Considering the model at the earlier study, geodesic angle variations at the bigger and smaller cross-sections with the increase of the height of the cone and variations of the number of circular ribs are shown in Fig. 5 and 6, respectively. As it is seen with the increase

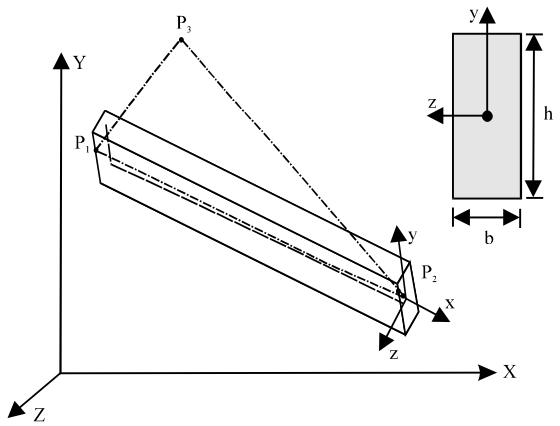

Fig. 4: A schematic of the beam element used in finite element analysis

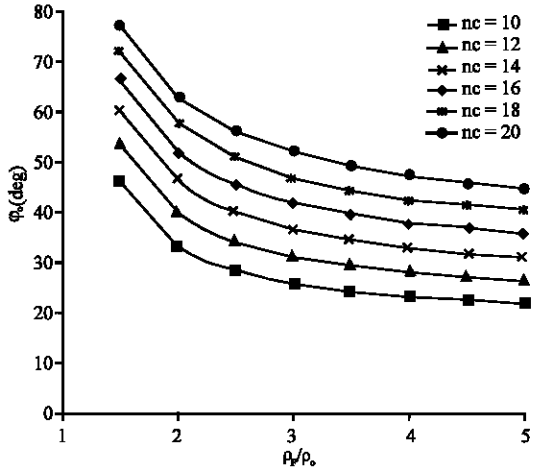

Fig. 5: Variation of φ_o with the increase of ρ_F/ρ_o ($\alpha = 34.7°$)

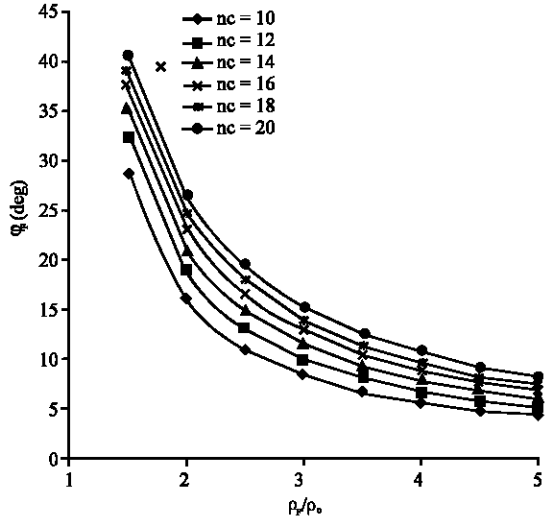

Fig. 6: Variation of φ_F with increase of ρ_F/ρ_o ($\alpha = 34.7°$)

of the height of the cone, geodesic angles are non-linearly decreasing. Also, with the increase of the number of circumferential ribs at the same geometric conditions, geodesic angles at each section are reduced. Results show that by increasing the number of circumferential ribs, variations of the geodesic angle at the bigger section are reducing with a more inclination, compared to the smaller section. Regarding the total geometric specifications of the conical structure, geodesic angle can be achieved at the bigger and smaller cross-sections for a certain number of helical and circular ribs from the diagrams of Fig. 5 and 6. For example for the conical lattice structure with 10 circular ribs and the ratio $\rho_F/\rho_o = 2$ of geodesic angle at the bigger and smaller cross-sections are 15.98 and 33.44, respectively. Also, variations of

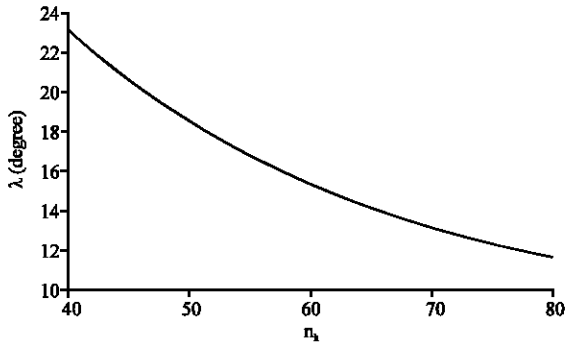

Fig. 7: Variation of λ with the increase of the number of helical ribs

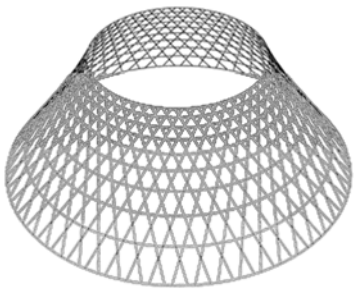

Fig. 8: Finite element model of the lattice conical shell, made by ABAQUS Software

λ with the increase of the number of helical ribs is shown in Fig. 7. The Finite Element Model with total specifications and geodesic angle is shown in Fig. 8.

VERIFICATION

Finite element model of the lattice conical shell which has undergone buckling analysis under axial and bending loadings in reference (Morozov *et al*., 2011) is used here and buckling analysis is performed on it using ABAQUS Software and Timoshenko's beam element. Geometric specifications and the materials used in the finite element analysis are chosen according to reference (Morozov *et al*., 2011). A schematic of the finite element analysis of the lattice conical shell with the defined geometric specifications is shown in Fig. 9. Critical loads here are in Newton and for better display of the deformation of the structure, the aspect ratio of 40 is applied.

Results presented in Table 1 show that the results achieved from the numerical finite element solution and the analytical results are of high accuracy. Regarding the verification performed in the following on the lattice conical and cylindrical structures with certain geometrical specifications and the equations stated earlier, weight optimization of the structure is performed.

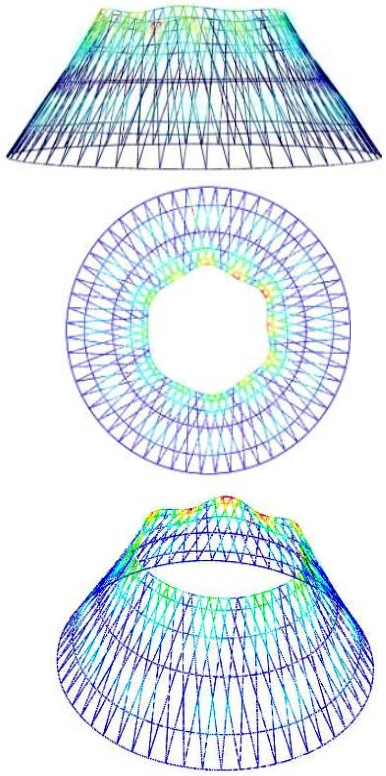

Fig. 9: Derivation of the critical buckling loading using finite element method (h = b = 4 mm, α = 5°)

Table 1: Comparison of the results of Morozov *et al.* (2011) with the results of analytical analysis and the numerical analysis presented here

	Numerical analysis		
Analytical analysis	h = 2 mm b = 8 mm	h = 4 mm b = 4 mm	h = 8 mm b = 2 mm
Morozov *et al.* (2011)	13.863	34.416	44.334
ABAQUS	15.030	33.831	49.112
Analytical	15.060	36.216	47.997

RESULTS AND DISCUSSION

Critical buckling load in structures depends upon stacking sequence of the ribs, angle of helical ribs, cross-section of the dribs, etc. Later in this study, results of variations of axial loading under clamped support conditions are investigated. Geometric specifications of the lattice conical shell are summarized in Table 2 with regards to Fig. 5 and 6. Also, the properties of materials used in the lattice conical shell are included in Table 3.

According to the diagram of Fig. 10, analytical results show that by increasing the a_c/a_hratio, critical buckling load increases.

Table 2: Geometric parameters of the lattice conical shell studied

b_h (mm)	b_c (mm)	H (mm)	α_*	α_f	n_h	n_c
5.75	4	18	33.44	15.98	53	10

Table 3: Properties of the materials used in the lattice conical shell

m_c (kg m^{-3})	E_c (GPa)	$\bar{\sigma}_h m_h$ (kg m^{-3})	(MPa)	E_h (GPa)
1410	64	1450	350	80

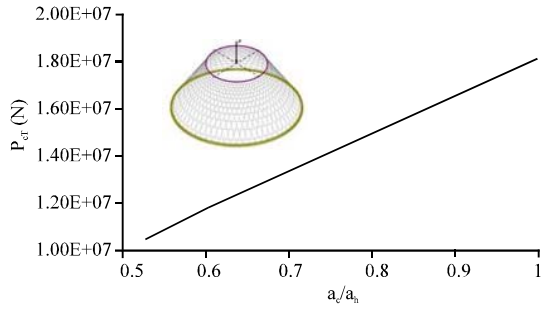

Fig. 10: Variation of buckling load versus increase of a_c/a_h

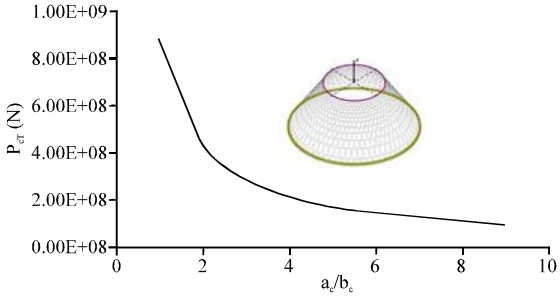

Fig. 11: Variation of critical buckling load versus increase of a_c/b_c ratio

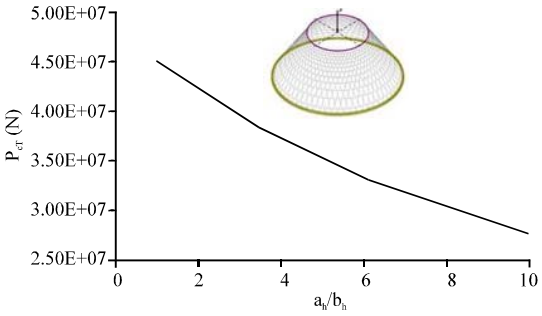

Fig. 12: Variation of critical buckling load versus increase of a_h/b_h ratio

Also, with the increase of a_c/b_c ratio, critical buckling load decreases (Fig. 11). Also, variations of the critical buckling load by increasing the ratio, non-linearly decreases (Fig. 12). In Fig. 13, variation of the critical buckling load versus increase of thickness has been shown for two states of analytical and Finite Element

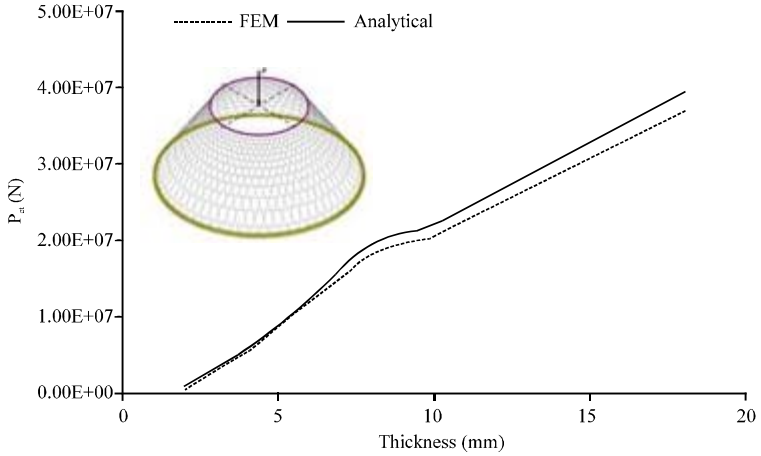

Fig. 13: Variation of critical buckling load versus increase of thickness of circular and helical ribs

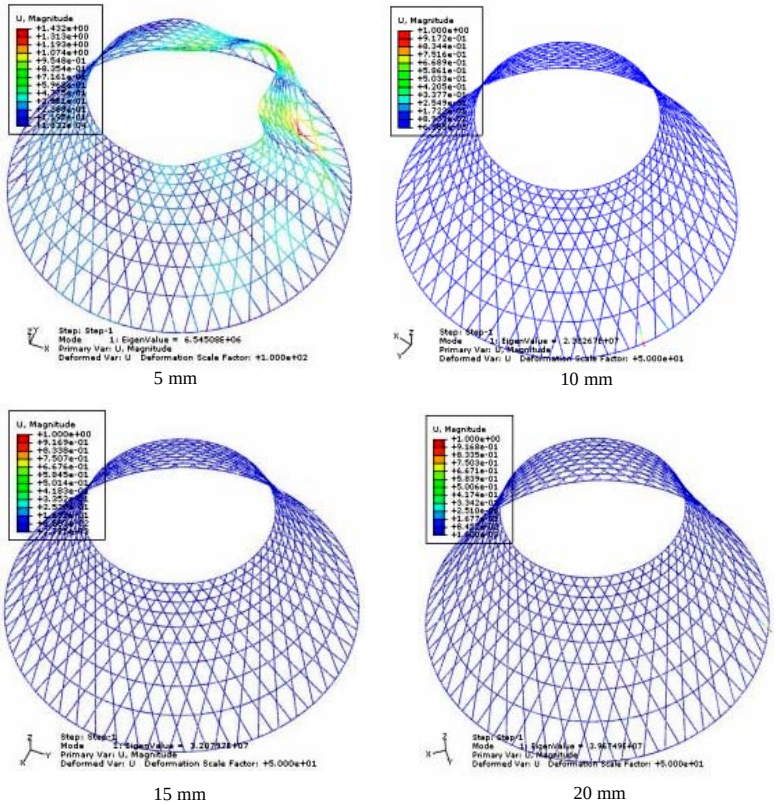

Fig. 14: A schematic of the first mode of buckling for the buckling of lattice conical shell under axial loading versus thickness variation of the rib (width = 5.75 mm)

Methods. Results indicate that by increasing the thickness of the ribs of lattice shell, the critical buckling load of the structure and non-linearly increases.

Regarding the diagram of Fig. 13, it is realized that with the increase of the thickness of the rib (approximately 20 mm), the beam element does not possess high accuracy in the convergence of the results of analytical and numerical analysis (Fig. 14). Also with the increase of the width of helical and circular ribs, critical buckling load increases non-linearly (Fig. 15).

Regarding the results presented, one can derive the critical axial load with a good accuracy using numerical

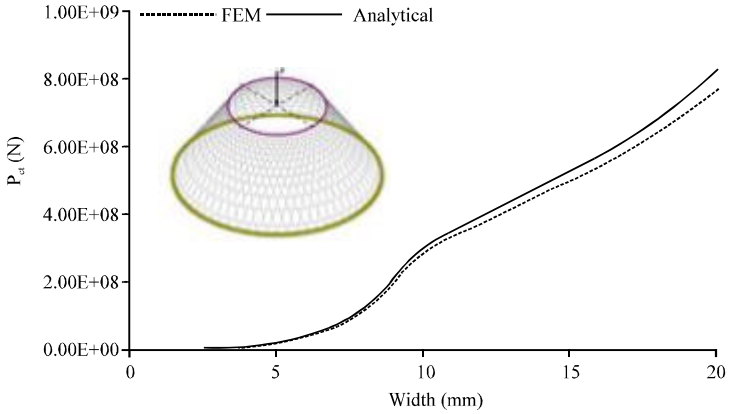

Fig. 15: Variation of critical buckling load versus increase of width of circular and helical ribs

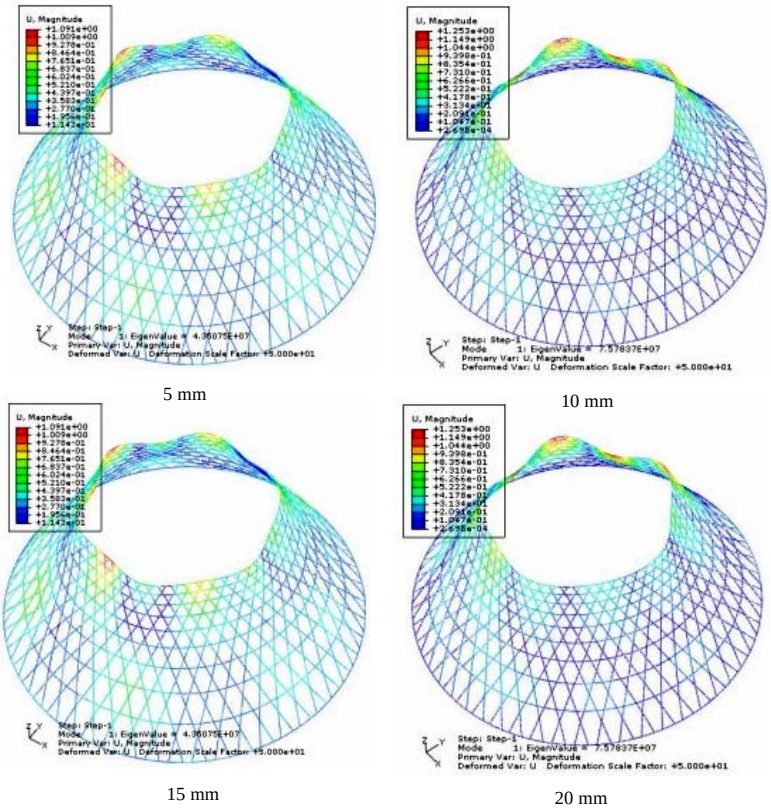

Fig. 16: First mode of buckling for the lattice conical shell under axial loading versus width variation of the rib (Thickness = 18 mm)

Finite Element Method and Analytical Method. A schematic of the first up to sixth modes of buckling of the lattice conical structure, under axial loading is shown in Fig. 16.

CONCLUSION

The study show that design of a lattice conical shell, requires considering different parameters. These parameters are independently chosen by the designer or are dependent. For buckling analysis of the lattice conical structure under axial loading, the equal stiffness of the shell in the axial, circumferential and through the thickness directions should be determined. Stiffness matrix of the lattice structure, besides the mechanical properties of helical and circular directions, depends upon the geometry of the cells of the lattice structure and also the angle of the helical ribs at different points of the

height. In buckling analysis of the lattice conical shell under axial loading, the following results are achieved:

- By increasing the a_c/a_h ratio, the critical buckling load increases
- By increasing the a_c/b_c ratio, the critical buckling load decreases
- By increasing the a_h/b_h ratio, the critical buckling load decreases
- By increasing the thickness of the circular and helical ribs, the critical buckling load increases non-linearly
- By increasing the width of the circular and helical ribs, the critical axial loading increases

REFERENCES

Balepin, V.V., M. Maita and S.N.B. Murthy, 2000. Third way of development of single stage to orbit ropulsion. J. Propulsion Ano Power, 16: 99-104.

Blom, A.W., S. Setoodeh, J.M.A.M. Hol and Z. Gurdal, 2007. Design of variable-stiffness conical shells for maximum fundamental eigenfrequency. Comput. Struct., 86: 870-878.

Goldfeld, Y. and J. Arbocz, 2004. Buckling of laminated conical shells taking into account the variations of the stiffness coefficients. AIAA J., 42: 642-649.

Goldfeld, Y., J. Arbocz and A. Rothwell, 2005. Design and optimization of laminated conical shells for buckling. Thin-Walled Struct., 43: 107-133.

Huybrechts, S. and T.E. Meink, 1996. Hybrid tooling for advanced grid stiffened structures (AGS). Proceedings of the Technical Conference, January 22-26, 1996, San Diego, CA., USA.

Huybrechts, S. and T.E. Meink, 1999a. Advanced grid stiffened structures for the next generation of launch vehicles. Proceedings of the Conference on Aerospace, Vol 1, February 1-8, 1997, Snowmass at Aspen, CO., pp: 263-270.

Huybrechts, S. and T.E. Meink, 1999b. Grid stiffened structures: A survey of fabrication, analysis and design method. Proceedings of the International Son Composite Materials, July 12-14, 1999, Plymouth, UK.

Kidane, S., G. Li, J. Helms, S. Pang and E. Woldesenbet, 2003. Buckling load analysis of grid stiffened composite cylinders. Composites Part B: Eng., 34: 1-9.

Kim, T.D., 1999. Fabrication and testing of composite isogrid stiffened cylinder. Compos. Struct., 45: 1-6.

Kim, T.D., 2000. Fabrication and testing of thin composite isogrid stiffened panel. Composite Structures, 49: 21-25.

Morozov, E.V., A.V. Lopatin and V.A. Nesterov, 2011. Finite-element modelling and buckling analysis of anisogrid composite lattice cylindrical shells. Compos. Struct., 93: 308-323.

Weingarten, V.I., E.J. Morgan and P. Seide, 1965. Elastic stability of thin-walled cylindrical and conical shells under axial compression. AIAA J., 3: 500-505.

Wodesenbet, E., S. Kidane and S.S. Pang, 2003. Optimization for buckling loads of grid stiffened composite panels. Compos. Struct., 60: 159-169.